ChemPubSoc Europe
DOI: 10.1002/cssc.201501446
CHEMSUSCHEM Full Papers

Efficient Conversion of Lignin to Electricity Using a Novel Direct Biomass Fuel Cell Mediated by Polyoxometalates at Low Temperatures

Xuebing Zhao[a, b, c] and J. Y. Zhu * [b, c]

A novel polyoxometalates (POMs) mediated direct biomass fuelcell (DBFC) was used in this study to directly convert lignin to electricity at low temperatures with high power output and Faradaic efficiency. When phosphomolybdic acid $H_3PMo_{12}O_{40}$ (PMo_{12}) was used as the electron and proton carrier in the anode solution with a carbon electrode, and 0_2 was directly used as the final electron acceptor under the catalyssis of Pt, the peak power density reached 0.96 $mWcm^{-2}$, 560 times higher than that of phenol-fueled microbial fuel cells (MFCs). When the cathode reaction was catalyzed by PMo_{12}, the power density could be greatly enhanced to 5 $mWcm^{-2}$. Continuous operation demonstrated that this novel fuel cell was promising as a stable electrochemical power source. Structure analysis of hte lignin indicated that the hydroxyl group content was reduced whereas the carbonyl group content increased. Both condensation and depolymerization takes place during the PMo_{12} oxidation of lignin.

Lignin is by far the most abundant aromatic material in nature. The pulp and paper industry alone produces millions of tons of technical grade lignin each year,[1] which is primarily combusted for heat and chemical recovery. Sustainable economic development requires efficient utilization of lignocellulosic biomass including lignin for clean energy and bio-products. Lignin has a good heating value higher than cellulose and hemicelluloses[2] and may be used for electricity generation through combustion or gasification to produce heat or gas fuels to drive steam or gas turbines. However, distributed operation at relatively small scales is preferred owing to the relatively lower energy density of lignin compared to gas fuels.

Fuel cells have attracted great interest in recent years as a clean, portable, and alternative electricity production technology suitable for a variety of applications. Lignin can potentially be used to produce electricity using solid oxide fuel cells (SOFCs), direct carbon fuel cells (DCFCs), and microbial fuel cells (MFCs). However, external processing is required to convert lignin to suitable fuels. For example, gasification of lignin to syngas is necessary for SOFCs,[3,4] or carbonization to biochar or blending with active carbon prior to fueling DCFCs[5-7] The requirement of external processing to convert lignin to gaseous fuels or biochar not only increases the complexity of the system but also greatly reduces exergy efficiency.[8,9] Furthermore, these two types of fuel cells need to be operated at high temperatures. Degradation of lignin to small-molecule phenolic compounds is necessary for MFCs, in which some aerobic bacteria can use the phenolic compounds as carbon sources and generate electricity at low temperatures,[10-12] but with low efficiency and power output. The reported power density of phenol-fueled MFCs is usually less than 0.0017 $mW cm^{-2}$.[10,13] Moreover, the high chemoselectivity for substrates, rigorous reaction conditions, and limited lifetime substantially hinder their application.[14]

Fuel cells that can directly convert lignin or lignocellulosic biomass to electricity are desirable and critical for efficient, portable, and low cost electricity production. However, without the use of catalysts lignin oxidation proceeds very slowly owing to the complex lignin structure. The noble metal catalysts (e.g., Pt, Ru, Pd), commonly used in the direct hydrogen- or alcohol-based proton-exchange membrane fuel cells, cannot completely catalyze the electro-oxidization of C-C bonds of lignin to CO_2 at low temperatures.[15] Potential catalysts must serve as a mediator to transfer electron from lignin to the oxidant. Electrochemically, the oxidation–reduction potential of a potential catalyst must be higher than that of the structural moieties of lignin but lower than those of the oxidants, so that the catalyst can be regenerated and reused.

Polyoxometalate (POM), which is a polyatomic ion consisting of three or more transition metal oxyanions linked together by shared oxygen atoms, has distinct properties such as robust oxidative degradation ability and great potential as an electron reservoir.[16] Previous studies have shown that POM can be a good electron-transfer catalyst for generating power from CO at room temperature[17] or producing synthesis gas from biomass carbohydrates such as cellulose and hemicelluloses.[18]

[a] Dr. X. Zhao
Department of Chemical Engineering
Tsinghua University
Beijing (P.R. China)

[b] Dr. X. Zhao, Prof. Dr. J. Y. Zhu
Department of Biological Systems Engineering
University of Wisconsin
Madison, WI (USA)
E-mail:jzhu@fs.fed.us

[c] Dr. X. Zhao, Prof. Dr. J. Y. Zhu
USDA Forest Service
Forest Products Lab
Madison, WI (USA)

Supporting Information for this article is available on the WWW under http://dx.doi.org/10.1002/cssc.201501446.

regenerated. And last, the cell can directly convert lignin to electricity without prior external processing to avoid high exergy loss.

$$\text{lignin-H}_n + \text{POM}_{ox} \rightarrow \text{oxidized lignin} + \text{H}_n\text{-POM}_{red} \quad (1)$$

$$O_2 + 4H^+ + 4e^- \xrightarrow{Pt} 2H_2O \quad (2)$$

Cell performance

POM is an oxidant as well as a Brønsted acid.[21,22] Thus, it serves as an electron and proton carrier during oxidative degradation of lignin. Several Keggin-type or non-Keggin-type POMs including $H_3PW_{12}O_{40}$, $H_4PVW_{11}O_{40}$, $K_5PV_2Mo_{10}O_{40}$, and $H_3PMo_{12}O_{40}$ (PMo_{12}) at concentration of 0.25 M were used to oxidize a commercial lignosulfonate (LS) D748 at 5 g L^{-1}. Apparent color changes were observed as the oxidation reaction proceeded, and the corresponding UV/Vis absorbance was increased in the wavelength range of 500–1000 nm (Figure S1). A clear characteristic absorption peak at around 750 nm was observed for the reduced PMo_{12}, which is known as molybdenum blue. When the H_n-POM_{red} was discharged using O_2 as the oxidant in the fuel cell at room temperature, the maximum power densities for $H_3PW_{12}O_{40}$, $H_4PVW_{11}O_{40}$, $K_5PV_2Mo_{10}O_{40}$, and PMo_{12} were 0.01, 0.004, 0.005, and 0.10 mW cm^{-2}, respectively. PMo_{12} obtained the highest power output (Figure 2a) with an open circuit voltage (OCV) of 200 mV. Generally, the POMs that can oxidize lignin must have a higher redox potential than the lignin moieties. Oxidative degradation was found to take place at potentials between 0.6 and 0.8 V for phenolic units and at approximately 1.0 V for nonphenolic units, while the O_2/H_2O redox potential is + 1.229 V.[16] Thus, the redox potential of the POM used should be in the range of 0.6–1.2 V to oxidize the phenolic structure of lignin and serve as an electron carrier in the fuel cell. Theoretically, the standard cell potential is less than 0.63 V based on the following cell reaction [Eq. (3)], where n is the number of electrons or protons that can be transferred from 1 molecule of POM_{red} to oxygen. However, according to the Nernst equation, the cell potential is dependent on temperature and reaction quotient, and the output power density is also dependent on the polarization of the cell:

$$n/4O_2 + H_n\text{-POM}_{red} \rightarrow \text{POM}_{ox} + n/2\,H_2O \quad (3)$$

The PMo_{12} concentration had a significant effect on the cell voltage and power density, as shown in Figure 2b. The maximum power density increased from 0.014 to 0.10 mW cm^{-2} when the PMo_{12} concentration was increased from 5 mM to 0.25 M. However, the effect of the concentration on the increase in power density was not only attributed to the increased concentration difference, but was largely attributed to the oxidation reaction kinetics of lignin by POMs, the high discharge rate of POMs on the electrode surface, and the high probability of POM_{red} discharge at the electrode. The cell reactions using PMo_{12} as the anode mediator and O_2 as the final electron acceptor can be written as follows:

(a) Lignin oxidation by PMo_{12}:

$$H_3PMo_{12}^{VI}O_{40} + \text{lignin-H}_n \xrightarrow{\Delta \text{ or } h\nu} H_{3+n}PMo_{12-n}^{VI}Mo_n^{V}O_{40} + \text{oxidized lignin} \quad (4)$$

where $n = 1$–8, is the number of electrons that one molecule of PMo_{12} can accept according to Ref. [23].

(b) Anode half-cell reaction:

$$H_{3+n}PMo_{12-n}^{VI}Mo_n^{V}O_{40} - n\,H^+ - n\,e^- \rightarrow H_3PMo_{12}^{VI}O_{40} \quad (5)$$

with Nernst equation for electrode potential of

$$E_{anode} = E^{\circ}_{anode} - \frac{RT}{zF}\ln\frac{a_{H_3PMo_{12}^{VI}O_{40}}}{a_{H_{3+n}PMo_{12-n}^{VI}Mo_n^{V}O_{40}} \cdot a_H^n} \quad (6)$$

(c) Cathode half-cell reaction

$$1/2\,O_2 + 2H^+ + 2e^- \xrightarrow{Pt} H_2O \quad (7)$$

with Nernst equation for electrode potential of

$$E_{cathode} = E^{\circ}_{cathode} - \frac{RT}{zF}\ln\frac{1}{(f_{O_2}/p_{O_2})^{1/2} \cdot a_H^2} \quad (8)$$

(d) Total cell reaction

$$n/4\,O_2 + H_{3+n}PMo_{12-n}^{VI}Mo_n^{V}O_{40} \rightarrow H_3PMo_{12}^{VI}O_{40} + n/2\,H_2O \quad (9)$$

with total cell potential of

$$E_{cell} = E_{cathode} - E_{anode} = E^{\circ}_{cell} - \frac{RT}{zF}\ln\frac{a_{H_3PMo_{12}^{VI}O_{40}}}{a_{H_{3+n}PMo_{12-n}^{VI}Mo_n^{V}O_{40}} \cdot (f_{O_2}/p_{O_2})^{n/4}} \quad (10)$$

Therefore, the electrode and cell potentials are influenced by H^+, PMo_{12}, and reduced PMo_{12} ($PMo_{12,red}$) activities (concentrations), and O_2 fugacity (partial pressure). Increasing the concentration of $PMo_{12,red}$ (or ratio of $PMo_{12,red}/PMo_{12}$) can enhance cell potential. Moreover, PMo_{12} also acts as the electrolyte in the cell, and a high PMo_{12} concentration can reduce the internal resistance of the cell and increase the output current density.

The power density of the cell was significantly influenced by the lignin concentration in the pre-oxidation system (Figure 2c), because the concentration of $PMo_{12,red}$ and the ratio $PMo_{12,red}/PMo_{12}$ were dependent on both the PMo_{12} and D748 concentration. Therefore, a higher D748/PMo_{12} ratio resulted in a higher cell voltage and power density. When 0.1 M PMo_{12} and 25 g L^{-1} D748 were used, the OCV of the cell reached 310 mV with maximal power density of 0.34 mW cm^{-2}. However, it should be noted that the observed effects of lignin concentration on the power density was actually reflected by the concentration of $PMo_{12,red}$ in the anode solution because lignin did

However, only very recently, a novel solar-induced hybrid fuel cell using POM as the photocatalyst and charge carrier was r e ported, with good levels of electricity current and power density production directly from lignocellulosic biomass at a low temperature without external chemical processing.[19,20] Moreover, a substantially higher power output was achieved than from cellulose-based MFCs. These results are very promising and exciting for the development of a direct lignocellulosic biomass fuel cell (DBFC). Here we report direct conversion of lignin to electricity. Our study is focused on: (1) directly using industrial technical grade lignin available in large quantities with substantial market excess; (2) using liquid oxidants to improve the cell's power output and avoid the use of noble metal catalysts in the cathode reaction; and (3) using a substantially larger active electrode area (40 cm^2) than the reported studies[19,20] to demonstrate the potential for scalability. Systematic studies of several parameters were conducted to achieve a high current and power output. The practical significance of the study lies in: (1) the renewability and abundance of readily available lignocelluloses; and especially (2) the direct utilization of industrial lignin, which exists in many pulp mills around the world because of the capacity limits of chemical recovery boilers.

Results and Discussion

Working principles of the cell

The structure and working principle of the novel lignin-fueled cell using O_2 as the final electron acceptor are shown in Figure 1. In the anode chamber, lignin is oxidized by oxidative POM (POM_{ox}) where the POMs are reduced. Electrons and H^+ are transferred from lignin to POM as shown in reaction(1). Heat or light irradiation can be used to facilitate the reaction. In the anode chamber, the reduced POM (H_n-POM_{red}) is further re-oxidized by O_2 through an external circuit, while the H^+ released from H_n-POM_{red} passes through the proton exchange membrane (PEM) into the cathode chamber, where it reacts with O_2 under the catalysis of Pt to form reduced products (H_2O), as shown in reaction(2). This novel DBFC has several merits. First, the cell can be operated under mild conditions with efficient electron transfer from lignin to oxidant. Second, the cell does not need to use expensive noble metals for anode catalysts because POM plays both roles as a catalyst and an electron carrier. POMs are much less expensive than noble metals such as Pt and very easy to prepare. Third, the POM is chemically and thermally very stable, and can be easily

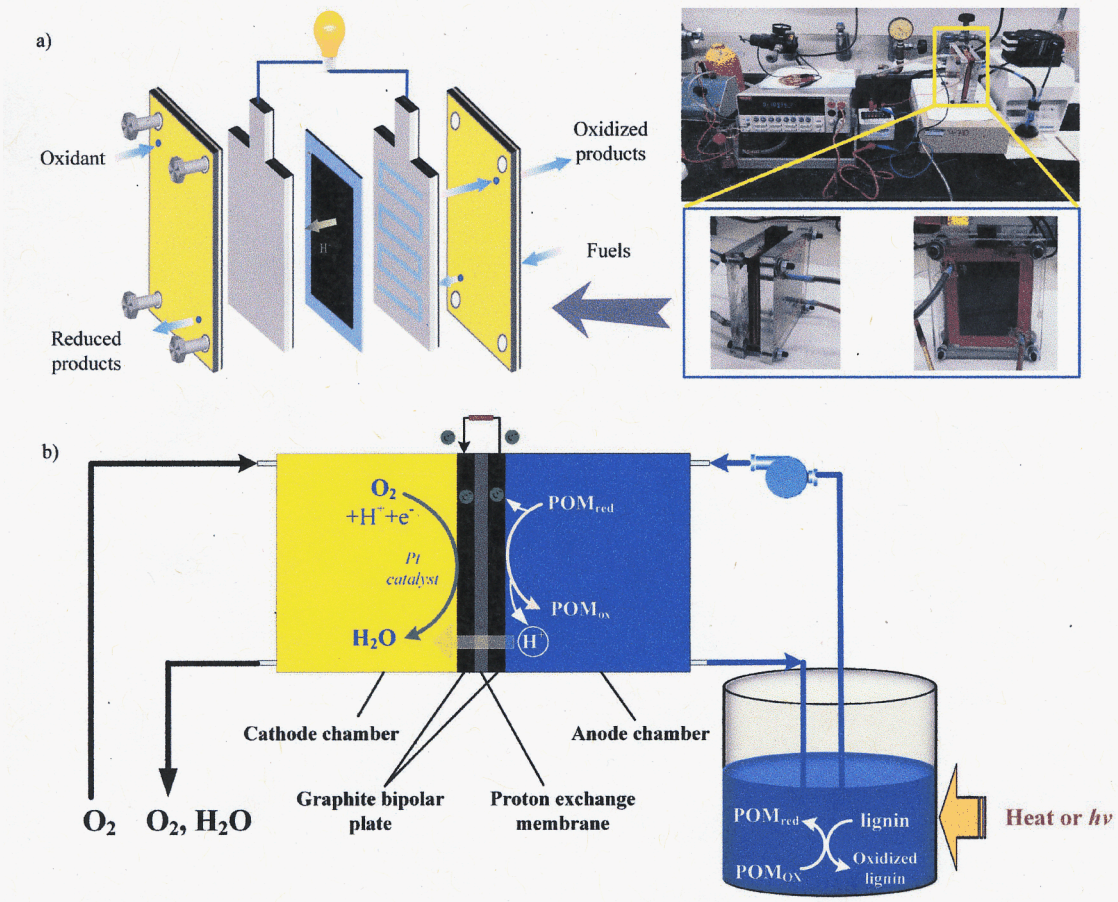

Figure 1. a) Structure of the POM-mediated direct biomass fuel cell. b) Schematic illustration of the working principle of the fuel cell directly using O_2 as the final electron acceptor.

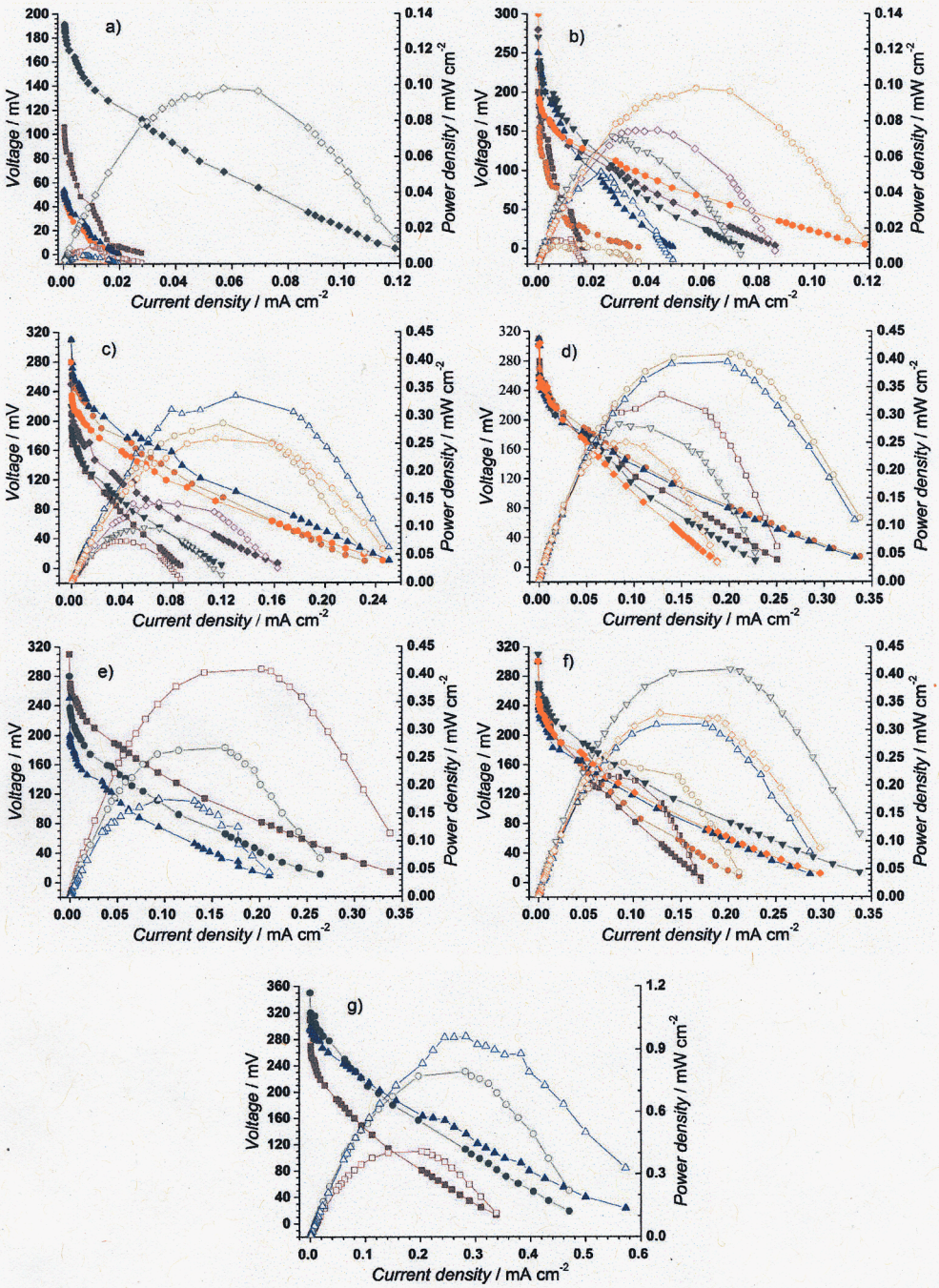

Figure 2. ■Output cell voltage (solid symbols) and power density (open symbols) of the fuel cell operated under different conditions using O_2 as the final electron acceptor. Pre-oxidation at 100 °C and discharging at 25 °C for a–f. a) Effect of POM type: ■ $H_3PW_{12}O_{40}$, ● $H_4PVW_{11}O_{40}$, ▲ $K_5PV_2Mo_{10}O_{40}$, ◆ $H_3PMo_{12}O_{40}$. b) Effect of PMo_{12} ($H_3PMo_{12}O_{40}$) concentration: ■ 0.005 M, ● 0.01 M, ▲ 0.02 M, ▼ 0.05 M, ◆ 0.1 M, ⬢ 0.25 M. c) Effect of D748 concentration: ■ 0.1 M $H_3PMo_{12}O_{40}$ + 5 g L^{-1} D748, ● 0.1 M $H_3PMo_{12}O_{40}$ + 15 g L^{-1} D748, ▲ 0.1 M $H_3PMo_{12}O_{40}$ + 25 g L^{-1} D748, ▼ 0.25 M $H_3PMo_{12}O_{40}$ + 5 g L^{-1} D748, ◆ 0.25 M $H_3PMo_{12}O_{40}$ + 15 g L^{-1} D748, ⬢ 0.25 M $H_3PMo_{12}O_{40}$ + 25 g L^{-1} D748. d) Effect of lignin type with total sample solids concentration of 25 g L^{-1}: ■ D748, ● KL, ▲ EHL, ▼ Na-LS, ◆ Ca-LS. e) Effect of salts at 25 °C: ■ Control, ● 10% Na^+, ▲ 10% Ca^+. f) Effect of H_3PO_4 concentration: ■ 0, ● 0.11 M, ▲ 0.24 M, ▼ 0.36 M, ◆ 0.47 M. g) Effect of temperature: ■ Ambient *T*, ,. 60 °C, 78 90 °C.

not directly take part in the cell discharge. Thus, the conditions for pre-oxidation of lignin by POMs might significantly impact the kinetics of electron and proton transfer to POMs. The cell performance was also found to be impacted by the type of lignin when the initial $PMo_{12,red}$ concentrations were the same, as shown in Figure 2d. Kraft lignin (KL) and enzymatic hydroly-

sis residue lignin (EHL), both not containing any free salts, showed much higher power density than D748 and the two SPORL spent liquors (containing Na-LS or Ca-LS), although the OCVs for the latter three lignin fuels were similar. This indicated that the presence of salts had negative effects on cell performance. Furthermore, Ca^{2+} had more negative influence than Na^{+}. To verify this fact, NaCl and $CaCl_2$ with a cation concentration of 10% (approximately the same as the concentration of Na+ or Ca^{2+} in the two SPORL spent liquors) were added into the anode chamber of the cell fueled by KL. As shown in Figure 2e, a substantial reduction in power density was observed after the addition of salts. Moreover, $CaCl_2$ indeed showed more negative effects than NaCl. The same phenomenon has been observed in proton exchange membrane fuel cells.[24] One possible explanation was the fouling of PEM by salts.[25] The metal ions (cations) may contaminate PEM thus limiting H^{+} conductivity of the membrane and increase the observed internal resistance of the cell. Some researchers have demonstrated that the sulfonate sites of the membrane had a higher affinity to most cations than protons, which resulted in a reduced conductivity of the membrane when a large amount of cations was replaced with protons.[26]

The H_3PO_4 concentration also had a significant effect on the power density of the fuel cell, as shown in Figure 2f. The maximal output power density increased from 0.22 to 0.41 $mWcm^{-2}$ when the H_3PO_4 concentration was increased from 0 to 0.36M. Further increasing the H_3PO_4 concentration to 0.47 M reduced the power density to 0.33 $mWcm^{-2}$, perhaps owing to the improved electron transfer from lignin to PMo_{12} as well as anodic reactions. However, a high H_3PO_4 concentration may degrade the PMo_{12} structure and thus reduce the power density.

Increasing the operating temperature from 25 to 90°C (temperature of the external vessel) resulted in an increase in the maximal power density from 0.41 to 0.96 $mWcm^{-2}$ (Figure 2g), because both the electrode reaction kinetics and proton conductivity of the membrane are dependent on temperature. High temperature promoted the reaction rates as well as proton conductivity of the PEM.[27]

Improving cell performance using liquid catalyst or oxidants for the cathodic reaction

Air and O_2 are relatively inexpensive oxidants with a great potential for large scale applications. However, a noble metal such as Pt is required as a catalyst. Another problem associated with an air or O_2 cathode is the mass transfer limitation because of the reaction taking place in a gas–liquid–solid triphase system. Therefore, processes for improving gas diffusion in the electrode are required to improve gas contact with the catalyst and reactants, which further increases the cost of the electrode. Intuitively, the cell performance can be improved by using a liquid catalyst or oxidant because of the higher reaction rate resulting from the higher mass transfer rate in liquid phase than in gas phase. The principles of the novel cell using a liquid catalyst or oxidant in cathode chamber are shown in Figure 3a. Similar to the anode chamber, the cathode was connected to an external vessel, where the liquid oxidant or catalyst was heated to a desired temperature. The liquid oxidant or catalyst was continuously pumped into the cathode chamber where it reacts with protons and electrons. When O_2 or air was used as the final electron acceptor, it was ventilated into the external vessel where electrons were transferred to O_2 from liquid catalyst such as the reduced PMo_{12} (Figure 3b). The reaction efficiency was thus improved by using this liquid catalyst.

The voltage and power density produced at 25 (Figure 4a) and 90°C (Figure 4b) using several liquid oxidants were compared to using air or O_2 directly under catalysis with Pt (termed as air or O_2 cathode here). As shown in Table 1, the air cathode produced an OCV of 210 mV with a P_{max} of 0.12 $mW\,cm^{-2}$ at 25°C. However, OCV and P_{max} increased to 310 mV and 0.41 $mWcm^{-2}$, respectively, when the O_2 cathode was used. Liquid catalysts such as POM were found to greatly facilitate the cathode reaction. When PMo_{12} was used alone, the OCV and P_{max} at 25 °C were 220 mV and 0.36 $mWcm^{-2}$, respectively; however, when PMo_{12} and O_2 were used together in the cathode chamber and the external vessel, the OCV and P_{max} at 25°C were 430 mV and 0.49 $mWcm^{-2}$, respectively. Stronger oxidants such as $KMnO_4$ greatly enhanced the voltage and power density; the OCV and P_{max} reached 680 mV and 3.63 $mW\,cm^{-2}$, respectively, when the discharge of the cell was performed at 25°C with 0.2 M $KMnO_4$.

The output power of the cell was also greatly enhanced at the elevated temperature of 90°C when a liquid oxidant or catalyst was used. The P_{max} reached 3.47 $mW\,cm^{-2}$ with an OCV of 460 mV when 0.1 M PMO_{12} was solely used as the electron acceptor in the cathode; however, the corresponding P_{max} and OCV reached 5.00 $mWcm^{-2}$, and 690 mV, respectively, when 0.1 M PMO_{12} and O_2 were used. This power was high enough to drive a small motor into fast motion, as observed in our experiments (see video in the Supporting Information). It was found that when PMo_{12} was solely used as the electron acceptor in the cathode chamber, the color of the cathode solution gradually changed from light yellow (color of PMo_{12}) to dark blue (color of $PMo_{12,red}$) as discharging proceeded (Figure S2A. Supporting Information). However, when O_2 was continuously ventilated to the external vessel of the cathode chamber, the color of the cathode solution was much lighter (Figure S2B). The UV/Vis absorption spectra shown in Figure S2 also corroborated that the $PMo_{12,red}$ concentration was much higher when PMo_{12} was solely used as the electron acceptor in the cathode. It indicated that O_2 could effectively re-oxidize the reduced PMo_{12} in the cathode vessel at the experimental condition to maintain PMo_{12} (the oxidized state) at a high concentration. Therefore, a high reaction rate can be maintained, resulting in a higher power density with the ventilation of O_2. Much higher power output was observed when 0.5M H_2O_2 (P_{max} of 13.0 $mWcm^{-2}$ and OCV of 410 mV) or 0.2 M $KMnO_4$ (P_{max} of 45.1 $mWcm^{-2}$ and OCV of 900 mV) were used (Figure 4c). The Faradaic efficiency (FE) of the cell was in the range of 85–100% depending on the oxidants and operation temperature (Table 1), indicating that the fuel cell can achieve a high discharging efficiency.

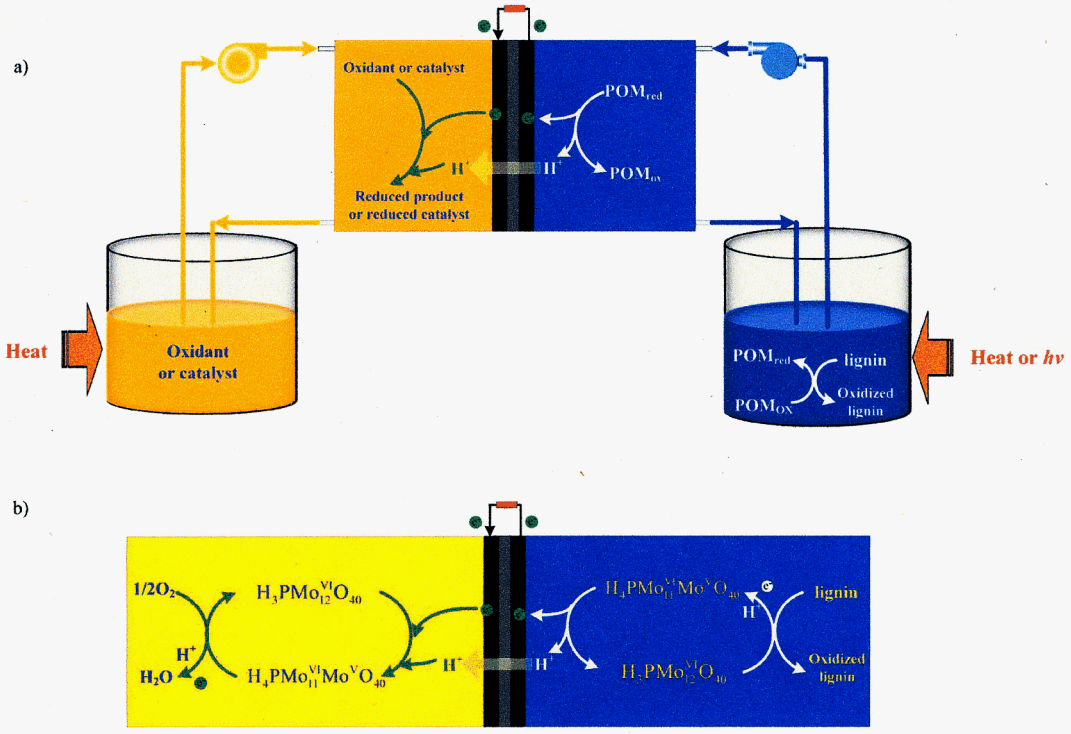

Figure 3. a) Principle of direct conversion of lignin to electricity with a liquid oxidant as the final electron acceptor or liquid catalyst as the electron mediator. b) Principle of direct conversion of lignin to electricity with oxygen (air) as the final electron acceptor and both cathodic and anodic reactions mediated by PMo_{12}.

The stability of the cell during continuous operation is shown in Figure 5. A relatively stable output was obtained with a current density of about 0.25, 0.4, and 0.5 $mAcm^{-2}$ (corresponding to 10, 16, and 20 mA of current, respectively), over a period of 420 min at an external resistance loading of 2 Ω when air, O_2 or $PMo_{12}+O_2$ was used as the electron acceptor. However, the current decreased continuously when $KMnO_4$ or $K_5PV_2Mo_{10}O_{40}+O_2$ were used as oxidant. This was mainly because of the difference between the cathodic and anodic reactions rates and the dependence of cell stability on reaction kinetics. A stable current can generally be obtained only when the cathodic and anodic reactions had similar reaction rates. It was found that when air or O_2 was used as the electron acceptor in the cathode, the $PMo_{12,red}$ concentration continuously increased, as indicated by the increased color (dark blue) of the anode solution and absorbance at 750 nm (Figure S3). This indicated that the kinetic rate of PMo_{12} reduction by lignin was higher than that of $PMo_{12,red}$ discharge (re-oxidation) by air or O_2 (the cathodic reaction). When a stronger oxidant such as $KMnO_4$ was used for discharge the $PMo_{12,red}$ concentration in the anode chamber was kept at a low level, owing to the much higher rate of the cathodic reaction (Figure 4a). Therefore, the output current was not stable and gradually decreased as the oxidant was consumed. The kinetics of the cell reactions need to be further investigated in more detail. However, the experimental results indicate that the novel direct biomass fuel cell with both the anodic and cathodic reactions catalyzed by PMo_{12} is promising as a stable electrochemical power source. Nevertheless, more optimization has to be performed to increase the power density.

Structure change of lignin

During PMo_{12} oxidation of KL, 23.2% of the lignin solids were depolymerized and solubilized into the aqueous phase. The low-molecular weight compounds identified in the solution are phenol derivatives such as benzoic acid, *p*-hydroxy benzaldehyde, vanillin, acetovanillone, vanillic acid, veratraldehyde, veratric acid, syringaldehyde, acetosyringone, and 2,6-dimethoxy-p-benzoquinone.[28] The hemicelluloses (xylan and mannan) content in the recovered solid was substantially reduced (Table 2). Similar results were also obtained when EHL was oxidized by PMo_{12}, ie., 20.5% of the solids were solubilized and the glucan and hemicellulose content decreased from 13.0% and 3.08% to 5.45% and 2.0996, respectively. The oxygen content of the oxidized lignin increased as evidenced by the new peak at 1705 cm^{-1} in the FTIR spectrum of the oxidized KL (Figure 6a) attributed to the carbonyl stretching in the carboxyl acid structures or unconjugated carbonyl structures of ketones and aldehyde.[29] The UV spectra of KL and oxidized KL shown in Figure 6b illustrate that the absorbance attributed to the benzene ring (λ_{max} at ~220, 250, and 280 nm) was somewhat weakened after PMo_{12} treatment, indicating that some benzene ring structures were destroyed. A redshift was observed for oxidized KL at a peak of approximately 220 nm in dioxane or 240 nm in a NaOH solution at pH 12. It demonstrat-

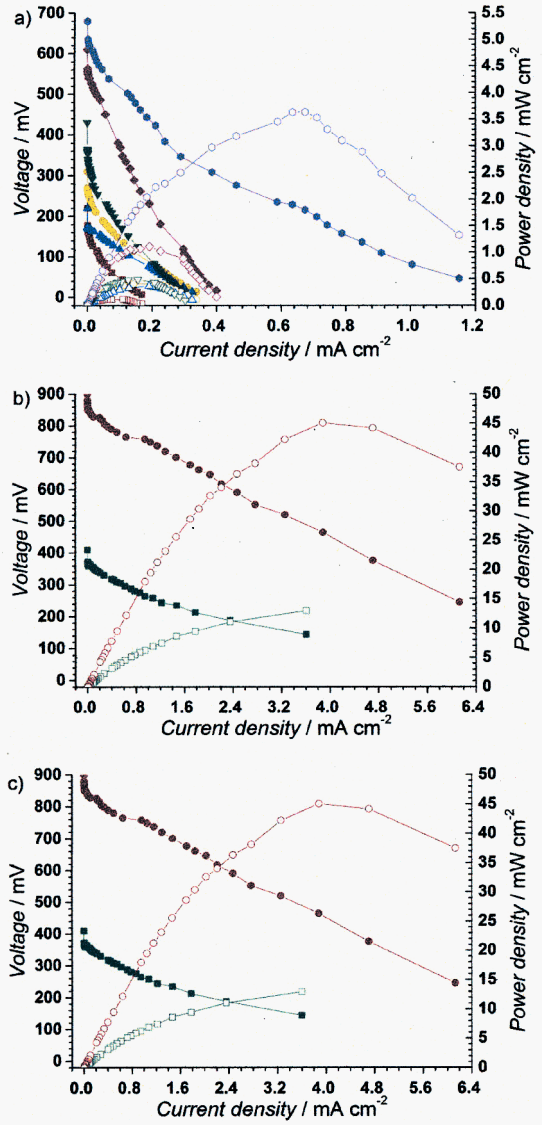

Figure 4. The voltage (solid symbols) and power density (open symbols) of the fuel cell with different oxidants; preoxidation was performed using 25 gL^{-1} KL at 100°C. a) at 25°C: ■ Air, ● O_2, ▲ 0.1 M $H_3PMo_{12}O_{40}$, ▼ 0.1 M $H_3PMo_{12}O_{40}+O_2$, ◆ 0.1 M $KMnO_4$, ⬢ 0.2 M $KMnO_4$. b) at 90 °C: ◙ Air, ● O_2, ▲ 0.1 M $H_3PMo_{12}O_{40}$, ▼ 0.1 M $H_3PMo_{12}O_{40}+O_2$, ★ 0.1 M $K_5PV_2Mo_{10}O_{40}$. c) at 90 °C: ⬢ 0.2 M $KMnO_4$ at PMo_{12} in anode and ■ 0.5 M H_2O_2 at PMo_{12} in anode.

ed that conjugation was formed with the benzene ring, probably by oxidation at the a-position (α-OH) to form a carbonyl structure.[28] ^{1}H NMR spectra (Figure 6c) of the samples showed that the signals of the aromatic proton (7.2–6.4 ppm), methoxyl group protons (4.15–3.00 ppm), phenolic OH (acetylated, 2.50–2.19 ppm), and aliphatic OH (acetylated, 2.19–1.58 ppm) for oxidized KL were weakened, indicating that a loss of aromaticity, demethylation, and the removal of aliphatic and phenolic hydroxyl groups took place during the PMo_{12} oxidation of KL. More evidence for the oxidation of KL was observed in the ^{1}H NMR spectrum of the oxidized KL, whereby the signal at 88 ppm was strengthened, which was attributed to the proton of the carboxyl or aldehyde groups. From the gel permeation chromatography (GPC) analysis (Figure 6d), it was found that the weight-average molecular weight (M_w) of the lignin sample increased from 3,350 (KL) to 10,080 (oxidized KL), but the number-average molecular weight (M_N) decreased from 1240 (KL) to 950 (oxidized KL), and corresponding polydispersity (M_w/M_N) increased from 2.70 (KL) to 10.61 (oxidized KL). These results demonstrated that both condensation and depolymerization of lignin took place during the oxidation of KL by PMo_{12},. Similar results have been reported by Kim et al.[30] when milled wood lignin (MWL) was oxidized by POMs.

POMs have distinct properties such as robust oxidative degradation ability and great potential as electron reservoirs.[16] They have been used for delignification and bleaching of lignocellulosic pulps. It has been found that POM treatment of lignin leads to a decrease in α-OH/β-O-4 inter-unit linkages[30] and an increase in quinone and α-carbonyl structures[16] An ideal POM as a catalyst for direct conversion of lignin to electricity should be strong enough to oxidize lignin to yield CO_2 and H_2O as the main final products and be re-oxidized by oxygen without loss of activity. However, complete oxidization of lignin is not possible under mild conditions owing to the presence nonphenolic moieties, which are difficult to be oxidized by POMs.[16] In the present work, PMo_{12} has been found to be a good catalyst and electron carrier to transfer electrons from lignin to oxygen. Although oxygen has a higher redox potential (higher oxidizing ability) than PMo_{12}, its direct reaction with lignin is very low without a catalyst. However, the reaction between PMo_{12} and lignin can proceed much more quickly when the reaction takes place in a solution or a liquid–solid system. Therefore, the PMo_{12} mediated lignin fuel cell demonstrated good performance for electricity generation. Moreover, POM has photocatalytic activity. As reported previously,[19] starch and lignocellulosic biomass could be oxidized by POM in solution under solar irradiation and easily re-oxidized by O_2 through an external circuit, with the production of electricity. Therefore, this novel DBFC is also a hybrid fuel cell combining solar energy conversion. Because POMs are usually tolerant to most organic and inorganic contaminants, unlike noble metal catalysts, they can be directly applied to almost any raw lignin feedstock without prior purification or cleaning.[20]

Air and oxygen are inexpensive oxidants for practical applications. However, noble metal catalysts such as Pt have to be used. Another problem associated with directly using air or pure oxygen as electron acceptor is the relatively low OCV. According to the standard electrode potential listed in Table 1, the thermodynamic cell potential of pure O_2 used for discharging is 0.73 V. However, the determined OCV of the cell at 90°C was only 0.35 V. Generally, the actual cell voltage is affected by losses from various electrochemical processes, mainly activation polarization, ohmic polarization, and concentration polarization,[31] as expressed by the equation

$$V_{act} = E_{rev} - IR_o - \eta_{cathode} - \eta_{anode} \quad (11)$$

Table 1. Effect of oxidants on OCV and maximal power density (P_{max}) at 25 °C and 90 °C.

Oxidant	OCV [mV]		P_{max}[a] [mW cm^{-2}]		FE[b] [%]		Cathode reaction	E° [V][c]
	at 25 °C	at 90 °C	at 25 °C	at 90 °C	at 25 °C	at 90 °C		
Air	210	220	0.12	0.32	90.4	89.0	$1/2\,O_2 + 2H^+ + 2e^- \xrightarrow{Pt} H_2O$	1.229
O_2	310	350	0.41	0.96	100.9	94.3	$1/2\,O_2 + 2H^+ + 2e^- \xrightarrow{Pt} H_2O$	1.229
0.1 M PMo_{12}	220	460	0.36	3.47	88.7	85.6	$2H_3PMo_{12}^{VI}O_{40} + 2H^+ + 2e^- \rightarrow 2H_4PMo_{11}^{VI}Mo^{VI}O_{40}$[d]	0.50[e]
0.1 M $PMO_{12} + O_2$	430	690	0.49	5.00	87.5	91.9	$2H_3PMo_{12}^{VI}O_{40} + 2H^+ + 2e^- \rightarrow 2H_4PMo_{11}^{VI}Mo^{VI}O_{40}$[d] $1/2\,O_2 + 2H_4PMo_{11}^{VI}Mo^{VI}O_{40} \rightarrow 2H_3PMo_{12}^{VI}O_{40} + H_2O$[d]	0.50[e]
0.1 M $KMnO_4$	610	ND[f]	1.11	ND[f]	89.8	ND[f]	$MnO_4^- + 4H^+ + 3e^- \rightarrow MnO_2 + H_2O$	1.70
0.2 M $KMnO_4$	680	900	3.63	45.1	90.5	89.2	$MnO_4^- + 4H^+ + 3e^- \rightarrow MnO_2 + H_2O$	1.70
0.5 M H_2O_2	ND[f]	410	ND[f]	13.0	ND[f]	91.6	$H_2O_2 + 2H^+ + 2e^- \rightarrow 2H_2O$	1.763
0.1 M $K_5PV_2Mo_{10}O_{40} + O_2$	ND[f]	330	ND[f]	0.41	ND[f]	73.8	$2PV_2^VMo_{10}O_{40}^{5-} + 2H^+ + 2e^- \rightarrow 2HPV^VV^{IV}Mo_{10}O_{40}^{5-}$[d] $1/2\,O_2 + 2HPV^VV^{IV}Mo_{10}O_{40}^{5-} \rightarrow 2PV_2^VMo_{10}O_{40}^{5-} + H_2O$[d]	1.000[e]

[a] Maximal output power density. [b] Faradaic efficiency determined after discharging for 7 h. [c] Standard half-cell potential (E°) data were obtained from Lange's Handbook of Chemistry. [d] Here, we only consider the scenario that 1 e^- is transferred from/to POM_{red}/POM. [e] Data obtained from Ref. [36]. [f] Not determined.

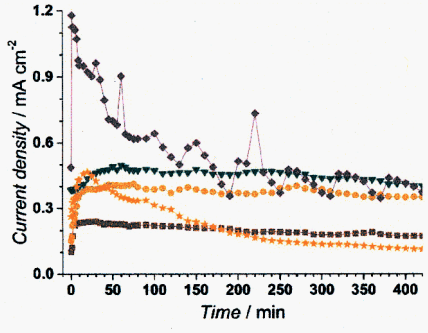

Figure 5. Continuous operation of the direct biomass fuel cell at 90°C with lignin fed every 2 h: ■ Air, ● O_2, ▼ 0.1 M $H_3PMo_{12}O_{40} + O_2$, ◆ 0.1 M $KMnO_4$, ★ 0.1 M $K_5PV_2Mo_{10}O_{40} + O_2$.

where E_{rev} is the Nernst potential of the reactants, I is the current through the cell, R_o is the ohmic resistance of the cell, and $\eta_{cathode}$ and η_{anode} are the cathodic and anodic polarization losses, respectively. It indicated that the potential loss of the cell was significant. The apparent internal resistance of cell determined by changing the external resistance loading was 12Ω, which was too large for practical applications of the cell. This internal resistance is caused by several aspects, but mainly attributed to the relatively low reaction rate in the cathode owing to the mass transfer limitation of oxygen permeating to the electrode surface. The power output could be dramatically enhanced when liquid oxidants such as H_2O_2 and $KMnO_4$ were used. This enhanced performance was mainly ascribed to the higher reaction rates of H_2O_2 and $KMnO_4$ with H^+ and electrons. The determined apparent internal resistances for the cells discharged with H_2O_2 and $KMnO_4$ were only 1–2Ω, much lower than those obtained using O_2. However, H_2O_2 and $KMnO_4$ are expensive for large-scale applications. Solid MnO_2, formed when $KMnO_4$ is used as the final electron acceptor, can precipitate in the pipe and on the electrode and PEM surface and reduce the fuel cell performance. Therefore, $KMnO_4$ is not a sustainable oxidant for large-scale applications, although it showed good cell performance in the experimental study. POM as a catalyst for cathode reactions greatly improves the cell efficiency. In the present work, when PMo_{12} was used as a catalyst with O_2 as the final electron acceptor, the power density reached 5 mWcm^{-2} on an electrode of area 40 cm^2, 2800 times higher than that of phenol-fueled MFCs.[10,13] Using a non-Keggin type $H_{12}P_3Mo_{18}V_7O_{85}$, a previous study achieved a power density of 51 mWcm^{-2} but only on an electrode active surface area of 1 cm^2, which was almost 3000 times higher than that of cellulose-based MFCs.[20] In the present work, the same POMs (PMo_{12}) were used as the catalyst in both anode and cathode reactions, which can avoid contamination of the electrode solution in case of leakage between the anode and cathode chambers. However, further investigation is needed to understand the kinetics of the cathodic and anodic reactions and dynamics of the cell discharging process.

Electrochemically, the potential of a fuel cell with both anodic and cathodic reactions mediated by PMo_{12} is dependent on the concentration ratio of $PMo_{12,red}/PMo_{12}$ because only $PMo_{12,red}$ and PMo_{12} are directly involved in the electrochemical reactions, as shown in Figure 3b. In this case, the theoretical standard potential of the cell is equal to zero because the electrodes are identical, which is similar to a concentration

Table 2. Chemical and elemental compositions of KL before and after POM oxidation (KL was oxidized by 0.1 M PMo_{12} at 100 °C with addition of 0.36 M H_3PO_4 for 7 h).

Sample	Amount of constituents [%]			Elemental composition [%]				
	glucan	xylan + mannan	lignin	C	H	O	N	Ph-OH
KL	0.58 ± 0.40	3.86 ± 0.48	88.4 ± 0.8	52.0 ± 0.11	5.19 ± 0.19	42.6 ± 0.18	0.23 ± 0.07	5.34 ± 0.10
oxidized KL	0.49 ± 0.09	0.13 ± 0.01	94.6 ± 2.0	50.17 ± 0.15	4.72 ± 0.04	44.80 ± 0.26	0.31 ± 0.05	4.33 ± 0.14

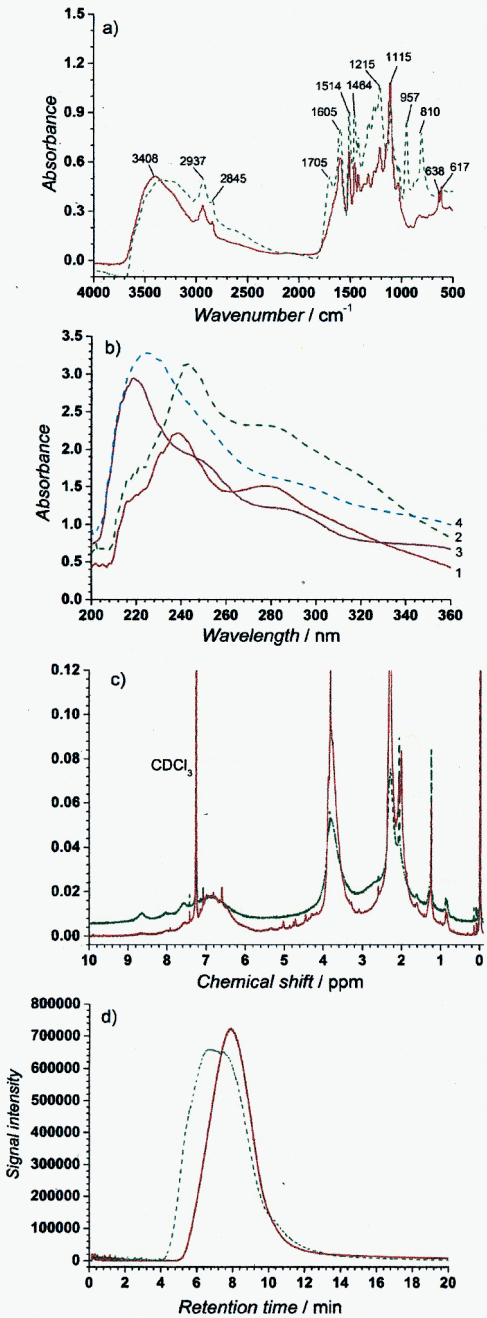

Figure 6. Analysis of KL structure before (solid lines —) and after (dashed tides-----) PMo12 oxidation by a) FTIR spectra. b) UV spectra 1,2: KL dissolved in 1,4-dioxane; 3.4: dissolved in NaOH pH 12. c) ^{1}H NMR spectra. d) Gel permeation chromatography (GPC).

cell. However, our experimental results showed that such a cell surprisingly demonstrated a good voltage and power density, especially at 90°C. The concentration differences of $PMo_{12,red}$ and H^+ between the anode and cathode contributed to the practical cell potential. Nevertheless, as the discharge proceeded, the concentration difference of $PMo_{12,red}$ became lower, and the cell's voltage and external current decreased. Therefore, to obtain a high voltage and power output, the $PMo_{12,red}$ concentration should be kept at a high level in the anode solution but at a low level in the cathode solution. For example, lignin has to be fed in batch or continuously to the anode solution to reduce the PMo_{12}, and the reduced PMo_{12} in the cathode has to be simultaneously reoxidized by oxidant such as O_2. Kinetically the concentrations of $PMo_{12,red}$ and PMo_{12} are significantly influenced by the lignin type, concentration, temperature, as well as the partial pressure of O_2, and thus the efficiency of the cell is greatly affected by these factors. Investigating the kinetics of the electrode reactions is important to optimize and improve cell performance.

As shown in Table 1, the FE of the cell was high. However, the electricity generation efficiency (EGE) from the fuel (lignin) needs further improvement. The KL used in the present work had a C, H, O, and N contents of 52.0%. 5.19%, 42.6%, and 0.23%, respectively. It can be calculated that theoretically, complete oxidation of 1 g KL to CO_2 and water results in the transfer of 0.172 mol electrons, corresponding to 16600 Coulombs of electric charge. The charge generated at 90°C with different oxidants after discharging for 7 h were in the range of 200-1000 Coulombs from 0.75 g KL, corresponding to an EGE of 1.6-8.0%. The EGE is dependent on the performance of the cell, but more importantly, on the reaction between POM and lignin. Some functional group present in lignin can be easily degraded by POM but others are difficult or cannot be oxidized under mild conditions. For example, the C-C bond is much more difficult to oxidize than -OH and a benzene ring. As found in the experiments, less than 25% of the lignin solid was dissolved into the aqueous phase under our experimental temperature (100°C for pre-oxidation), reaction time (7 h), and POM concentration (<0.25 M). increasing the pre-oxidation temperature and POM/lignin ratio might increase the dissolution of solid lignin. The remaining solid showed a higher M_w but lower M_N. It was found that POM oxidation involved side chains (such as α-OH/β-O-4) oxidation, degradation of some inter-unit linkages,[30] partial degradation of the benzene structure to form benzoquinone,[16] and removal of the aliphatic and phenolic hydroxyl groups. However, further oxidation of the degradation products by POM becomes more difficulty. The incomplete oxidation of lignin by POM under the condition of the present work is a limiting step to improve the lignin-to-electricity conversion efficiency. Therefore, the efficiency of electron transfer from lignin to POM, particularly complete oxidation of lignin, has to be further improved to increase the cell performance and sustainability.

Conclusions

Compared with conventional proton exchange membrane fuel cells (PEMFCs), the cell reported in this work still has to be further optimized to increase the power output. PEMFCs fueled by hydrogen or low-molecular-weight alcohols have been successfully commercialized after many years of development. Nowadays, depending on the operating conditions the power density of H_2-fueled PEMFC can reach 700 mWcm^{-2} or higher,

which is much higher than that of this work. However, it should be noted that conventional PEMFC cannot be fueled directly with polymeric biomass such as lignin, because the biomass polymer is difficult to oxidize at low temperatures even with noble metal catalysts. In this work, POM was introduced as a mediator to facilitate electron and proton transfer from lignin to oxygen, resulting in the conversion of lignin to electricity. However, more investigations on the operating conditions, kinetics, electrode materials, cell design, and assembly have to be done to enhance the power output, efficiency as well as operation stability.

Experimental Section

Materials

The POMs used in the experiments including $H_3PW_{12}O_{40}$, $H_4PVW_{11}O_{40}$, $K_5PV_2Mo_{10}O_{40}$, and $H_3PMo_{12}O_{40}$ (PMo_{12}) were previously prepared in our lab or purchased from Sigma Aldrich (St. Louis, MO, USA). The lignin samples evaluated included: (1) a commercial sodium lignosulfonate (LS) (D748) provided gratis by LignoTech USA (Rothschild, WI, USA).; (2) a Kraft lignin (KL) from Kraft pulping of a poplar wood from our laboratory; (3) an enzymatic hydrolysis lignin residue (EHL) derived from enzymatic hydrolysis of a SPORL pretreated poplar;[32] and (4) two spent liquors from SPORL pretreatment of a lodgepole pine[33] and a Douglas-fir forest harvest residue.[34] that contained mainly small molecular weight lignosulfonate (Na-LS in the lodgepole pine sample and Ca-LS in the Douglas-fir forest residue) and soluble sugars. The detailed chemical compositions of these lignin samples are listed in Table 3.

Assembly of the fuel cell

The structure of the novel POM-mediated DBFC is shown in Figure 1 a, which is similar to that reported previously[19] but with a much larger active electrode area (40 cm^2). The cell is composed of two graphite bipolar plates as anode and cathode electron collectors. The inner side of each bipolar plate had several 4 mm wide, 80 mm long, and 2 mm deep flow channels with a total active area of 40 cm^2. A membrane electrode assembly (MEA) (purchased from FuelCellsEtc, TX, USA) was sandwiched between the two bipolar plates to separate the fuel cell into an anode chamber and a cathode chamber. The MEA consisted of a Nafion 117 polymeric proton exchange membrane, an anode made of carbon cloth, and a cathode with carbon cloth loaded with Pt (60%)-C catalyst (5 mg cm^{-2}).These bipolar plates and MEA were further sandwiched by two acrylic plastic end plates. A rubber gasket was used between the bipolar plate and MEA to prevent leakage. The anode or cathode chamber were connected by Teflon pipes with external vessels containing fuels and POMs or O_2 cylinders.

Pre-oxidation of lignin by POMs

POM (5 mM-4.25 M) was used to prepare a 30 mL solution using deionized (DI) water in a 100 mL triangular flask connected with a condenser. Solid lignin (0.15–0.75g) was added into the POM solution for pre-oxidation. Concentrated H_3PO_4 (0.75 mL, 85 wt%) was added to the mixture and the flask was immersed in a glycerol bath at 100°C for 7 h. Electromagnetic stirring was used to obtain a homogeneous system. The color of the solution quickly turned dark blue. Samples were taken at regular intervals and diluted by 10–500times for UV/Vis absorption analysis.

Discharging of reduced POMs

The reduced POM solution was continuously circulated through an external glass vessel at a flow rate of 12 mL min^{-1} by a peristaltic pump. The vessel was immersed in a glycerol bath heated to the desired temperature of 90°C. The cathode chamber was supplied with O_2 as oxidant from a pressurized cylinder using Teflon pipes. Similarly, other liquid oxidants were used by continuously circulating them into the cathode chamber. An external resistance of 2 Ω was loaded between the cathode and anode graphite felts. Voltage on the external resistance was determined by a Keithley 2700 precision data acquisition system (Keithley Instruments Inc., USA). For continuous operation, after preheating for 5 min, the mixture was pumped into the anode chamber at a flow rate of 12 mL min^{-1}. KL (0.1 g) was fed into the vessel every 2 h.

Table 3. Chemical compositions of the lignin samples investigated.

Component	Lignin		
	D748	KL	EHL
Content of Solid lignin [%]			
glucan	0.26 ± 0.11	0.58 ± 0.40	13.04 ± 1.53
xylan + mannan	1.33 ± 0.11	3.86 ± 0.48	3.08 ± 0.13
acid soluble lignin		9.21 ± 0.50	3.71 ± 0.62
klason lignin		79.22 ± 0.26	72.37 ± 2.45
lignosulfonate	≈95	0	0
Amount of lignin-containing liquor [g L^{-1}]	Na-LS	Ca-LS	
lignosulfonate as Klason lignin	≈22	≈40	
acetic acid	4.29	3.18	
HMF	0.84	0.35	
furfural	0.96	1.13	
arabinose	0	1.47	
galactose	8.24	5.88	
glucose	12.58	9.40	
xylose	13.15	8.54	
mannose	27.75	20.64	

Analytical methods

The absorption spectra of the POM solutions were recorded on a UV/Vis spectrophotometer (Model 8453, Agilent Technologies, Palo Alto, USA). The electron transfer efficiency and reduction degree of PMo_{12} was analyzed according to a previous study[19] After the cell was discharged for 20–30 min to reach a relatively steady state, the current density was determined by measuring the voltages generated by the fuel cell with a variable external resistance loading changing from 1 to 10000 Ω[17] within 30 min. The FE (ε_F) of the cell mediated by $H_3PMo_{12}O_{40}$ (PMo_{12}) was calculated by the following equation:[19]

$$\varepsilon_F = \frac{Q_{discharge}}{Q_{PMo_{12}}} = \frac{\int_0^t Idt}{nFVC_{PMo_{12}}} \quad (12)$$

where $Q_{discharge}$ is the experimental charge quantity calculated from the discharge current–time curve, and Q_{PMo12} is the charge quantity released by reduced PMo_{12} calculated by spectrophotometry; I is the electric current determined during the discharging process, A; n is number of electrons obtained per Keggin unit of PMo_{12}; C_{PMo12} is the concentration of PMo_{12}, molL^{-1}; V is the volume of electrolyte solution, L; and F is the Faraday constant, 96485 Cmol^{-1}.

The chemical compositions and structural features of lignin and oxidized lignin including elementary compositions and functional groups were analyzed by UV spectroscopy, FTIR spectroscopy, ^{1}H NMR spectroscopy, and gel permeation chromatography (GPC) according to our previous work.[35]

Acknowledgements

Authors are grateful to Prof Yulin Deng and Dr. Wei Liu at Georgia Institute of Technology for their expertise, helping us set up the fuel cell, and many scientific discussions. The authors would also like to acknowledge Rolland Gleisner of the US Forest Service, Forest Products Laboratory, for technical support in setting up the fuel cell. This work was conducted when X.Z. was a visiting scientist at the US Forest Service, Forest Products Lab, and on official government time of J.Y.Z.

Keywords: direct biomass fuel cells · lignins · phosphomotybdic acids · polyoxometalates · power density

[1] F. Calvo-Flores, J. Dobado, *ChemSusChem* **2010,** *3,* 1227-1235.
[2] A. Demirbas, *Energy Convers. Manage.* **2001,** *42,* 183-188.
[3] J. Karl, N. Frank, S. Karellas, M. Saule, U. Hohenwarter, *J. Fuel Cell Sci. Technol.* **2009,** *6,* 021005.
[4] C. Athanasiou, F. Coutelieris, E. Vakouftsi, V. Skoulou, E. Antonakou, G. Marnellos, A, Zabaniotou, *Int. J. Hydrogen Energy* **2007,** *32,* 337-342.
[5] R. Lima, R. Raza, H. Qin, J. Li, M. Lindstrom, B. Zhu. *RSC Adv.* **2013,** *3,* 5083 - 5089.
[6] A. Elleuch, A. Boussetta, J. Yu, K. Halouani, Y. Li, *Int J. Hydrogen Energy* **2013,** *38,* 16590-16604.
[7] J. Yu, Y. Zhao, Y. Li, *J. Power Sources* **2014,** *270,* 312-317.
[8] R. El-Emam, I. Dincer, G. Naterer, *Int. J. Hydrogen Energy* **2012,** *37,* 1689-1697.
[9] L. E. Arteaga-Pérez, Y. Cams-Ledon, R. Perez-Bermudez, L. M. Peralta, J. Dewulf, W. Prins, *Chem. Eng. J.* **2013,** *228,* 1121-1132.
[10] H. Luo, G. Liu, R. Zhang, S. Jin, *Chem. Eng. J.* **2009,** *147,* 259-264.
[11] H. Friman, A. Schechter, Y. Ioffe, Y. Nitzan, R. Cahan, *Microb. Biotechnol.* **2013,** *6,* 425-434.
[12] A. Borole, C. Hamilton, D. Schell, *Environ. Sci. Technol.* **2013,** *47,* 642-648.
[13] T. S. Song, X. Y. Wu, C. C. Zhou, *Bioprocess Biosyst. Eng.* **2014,** *37,* 133-138.
[14] F. Ahmad, M. Atiyeh, B. Pereira, G. Stephanopoulos, *Biomass Bioenergy* **2013,** *56,* 179-188.
[15] A. Brouzgou, A. Podias, P. Tsiakaras, *J. Appl. Electrochem.* **2013,** *43,* 119-136.
[16] A. Gaspar, J. Gamelas, D. Evtuguin, C. Neto, *Green Chem.* **2007,** *9,* 717-730.
[17] W. Kim, T. Voitl, G. Rodriguez-Rivera, J. Dumesic, *Science* **2004,** *305,* 1280-1283.
[18] B. B. Sarma, R. Neumann, *Nat. Commun.* **2014,** *5,* 4621.
[19] W. Liu, W. Mu, M. Liu, X. Zhang, H. Cai, Y. Deng, *Nat Commun.* **2014,** *5,* 3208.
[20] W. Liu, W. Mu, Y. Deng, *Angew. Chem. Int Ed.* **2014,** *53,* 13558-13562; Angew. Chem. **2014,** *126,* 13776-13780.
[21] J. Macht, M. Janik, M. Neurock, E. Iglesia, *Angew. Chem. Int. Ed.* **2007,** *46,* 7864-7868; *Angew. Chem.* **2007,** 119, 8010-8014.
[22] J. Macht, M. Janik, M. Neurock, E. Iglesia, *J. Am. Chem. Soc.* **2008,** *130,* 10369- 10379.
[23] H. Zhang, T. Wu, X. Yan, Y. Leng, S. Li, *Chem. J. Chin. Univ.* **1990,** *11,* 1096-1101.
[24] W. Yan, H. Chu, Y. Liu, F. Chen, J. Jang, *Int. J. Hydrogen Energy* **2011,** *36,* 5435-5441.
[25] J. Xu, G.P. Sheng, W. H. Luo, W. W. Li, L. F. Wang, H. Q. Yu, *Water Res.* **2012,** *46,* 1817-1824.
[26] T. Springer, B. Kienitz in *Proton Exchange Membrane Fuel Cells: Contamination and Mitigation Strategy* (Eds.: H. Li, S. Knights, Z. Shi, J. Van Zee, J. Zhang). CRC Press, Boca Raton, FL, **2010,** pp. 293-338.
[27] Y. Sone, P. Ekdunge, D. Simonsson, *J. Electrochem. Soc.* **1996,** *143,* 1254-1259.
[28] B. Bujanovic, S. Ralph, R. Reiner, K. Hirth, R. Atalla, *Materials* **2010,** *3,* 1888-1903.
[29] B. Bujanovic, R. Reiner, S. Ralph, R. Atalla, *J. Wood Chem. Technol.* **2011,** *31,* 121-141.
[30] Y. Kim, H. Chang, J. Kadla, *J. Wood Chem. Technol.* **2007,** *27,* 225-241.
[31] P. Cowin, C. Petit, R. Lan, J. Irvine, S. Tao, *Adv. Energy Mater.* **2011,** *1,* 314-332.
[32] J. Zhang, F. Gu, J. Zhu, R. Zalesny, *Bioresour. Technol.* **2015,** *186,* 223-231.
[33] H. Zhou, J. Y. Zhu, R. Gleisner, X. Qiu, E. Horn, J. Negrón, *Holzforschung,* 2015, DOI: 10.1515/hf-2014-0332.
[34] J. Zhu, M. Chandra, F. Gu, R. Gleisner, R. Reiner, J. Sessions, G. Marrs, J. Gao, D. Anderson, *Bioresour. Technol.* **2015,** *179,* 390-397.
[35] X. Zhao, D. Liu, *Ind. Crops Prod.* **2010,** *32,* 284-291.
[36] A. Bard, R. Parsons, J. Jordan, *Standard Potentials in Aqueous Solution,* CRC Press, 1985, pp. 480.

Received: October 26, 2015
Revised: November 13, 2015
Published online on December 22, 2015

CHEMISTRY & SUSTAINABILITY

CHEMSUSCHEM

ENERGY & MATERIALS

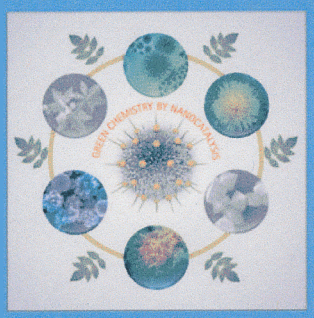

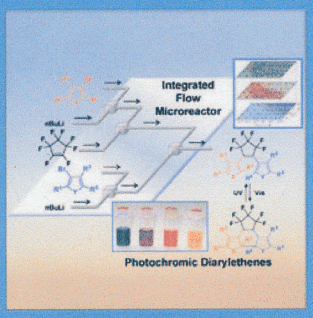

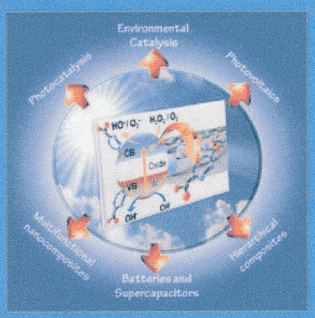

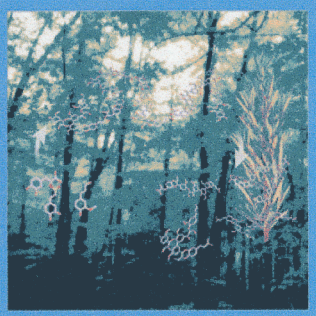

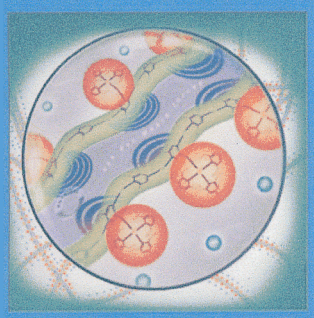

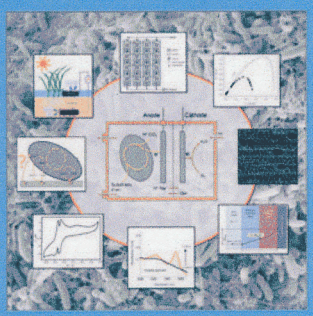

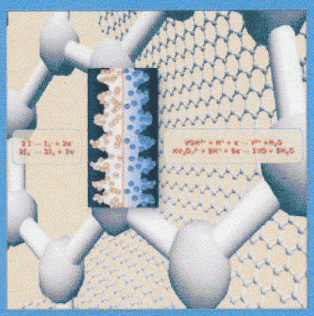

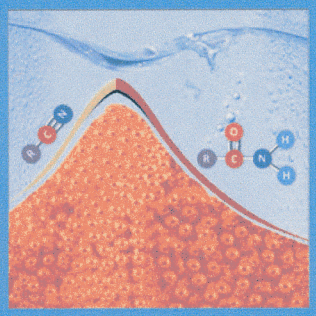

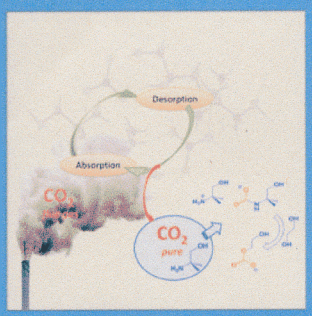

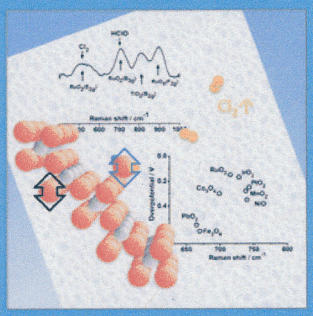

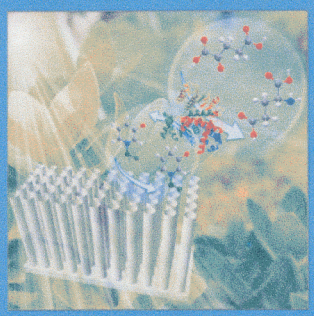

Reprint

A Journal of
ChemPubSoc Europe

WILEY-VCH

www.chemsuschem.org

Table of Contents

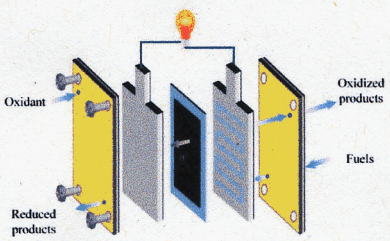

POMs full of energy! Polyoxometalates (POMs) mediated direct biomass fuel cells (DBFC) are used to directly convert lignin to electricity at low temperatures with high power output and Faradaic efficiency. Continuous operation demonstrated that the fuel cells are promising as a stable electrochemical power sources. Both condensation and depolymerization took place during the POM oxidation of lignin.

WILEY-VCH